arXiv:hep-ph/9811416v1 20 Nov 1998

Associated $J/\psi+\gamma$ production through double Pomeron exchange : The nature of the Pomeron and hard diffractive factorization breaking

Jia-Sheng Xu

Department of Physics, Peking University, Beijing 100871, China

Hong-An Peng

China Center of Advance Science and Technology (World Laboratory), Beijing 100080, China
and Department of Physics, Peking University, Beijing 100871, China

Abstract

We present a study of associated $J/\psi+\gamma$ production through double Pomeron exchange at energies reached at the Fermilab Tevatron and CERN LHC based on the Ingelman-Schlein model for hard diffractive scattering and the factorization formalism of nonrelativistic QCD for quarkonia production. We find that this process ($p+\bar{p}\rightarrow p+\bar{p}+J/\psi+\gamma+X$) can be used to probe the gluon content of the Pomeron and study the nature of hard diffractive factorization breaking.

PACS number(s): 12.40Nn, 13.85.Ni, 14.40.Gx

Typeset using REVTEX

In high-energy strong interactions the Regge trajectory with a vacuum quantum number, the Pomeron, plays a particular and very important role in soft processes in hadron-hadron collisions [1]. However, the nature of the Pomeron and its interaction with hadrons remain a mystery. Ingelman and Schlein [2] pointed out that hard diffractive scattering processes would give new and valuable insight about the nature of the Pomeron. It is assumed that the Pomeron, similar to the nucleon, is composed of partons, mainly of gluons, and the hard diffraction can be studied in a factorized way: First, the Pomeron is emitted from the diffractively scattered hadron, then one parton of the Pomeron takes part in hard subprocesses. Therefore, the partonic structure of the Pomeron could be studied experimentally. The Pomeron has a partonic structure was confirmed subsequently by various experiments [3–6].

However, there is an important problem, the factorization problem. The Ingelman and Schlein (IS) model for hard diffraction is based on the assumption of hard diffractive scattering factorization. Recently, a factorization theorem has been proven by Collins [7] for the lepton induced hard diffractive scattering processes, such as diffractive deep inelastic scattering (DDIS) and diffractive direct photoproduction of jets. In contrast, no factorization theorem has been established for hard diffraction in hadron-hadron collisions. At large $|t|$ (t is the square of the hadron's four-momentum transfer), where perturbative QCD applies to the Pomeron, it has been proven that there is a leading twist contribution which breaks the factorization theorem for hard diffraction in hadron-hadron collision [8]. This coherent hard diffraction was observed by the UA8 Collaboration in diffractive jet production, in this experiment t is in the region $-2 \leq t \leq -1$ GeV^2 [3]. On the other hand, for the Pomeron at small $|t|$, nonperturbative QCD dominates, it is unclear whether hard diffractive factorization is valid or not in hadron-hadron collisions. In phenomenology, the large discrepancy between the theoretical prediction and the Tevatron date on the diffractive production of jets and weak bosons, *at al.*, signals a breakdown of hard diffractive factorization in hadron-hadron collisions [9], but the nature of hard diffrative factorization breaking is still unclear.

In a previous paper, we have studied associated $J/\psi+\gamma$ production in single diffractive (SD) scattering at the Fermilab Tevatron and CERN LHC energies based on the IS model for hard diffractive scattering and the nonrelativistic QCD (NRQCD) factorization scheme for quarkonia production [10]. In this BRIEF REPORT, we complete our study of associated $J/\psi+\gamma$ diffractive production by discuss associated $J/\psi+\gamma$ production at large P_T through double Pomeron exchange (DPE):

$$p(P_p) + \bar{p}(P_{\bar{p}}) \rightarrow p(P'_p) + \bar{p}(P'_{\bar{p}}) + J/\psi(P) + \gamma(k) + X. \tag{1}$$

This process is of special interesting because the large P_T J/ψ produced is in the central rapidity region and is easy to be detected through its leptonic decay modes, and the J/ψ's large P_T is balance by the associated high energy photon. We will see the measurement of this process at the Tevatron and LHC would shed light on the nature of the Pomeron and the hard diffractive factorization breaking. Furthermore, this process is also interesting to the study of heavy quarkonium production mechanism, and the P_T smearing effects.

Within the NRQCD framework [11,12] J/ψ is described in terms of Fock state decompositions as

$$|J/\psi\rangle = O(1)\ |c\bar{c}[^3S_1^{(1)}]\rangle + O(v)|c\bar{c}[^3P_J^{(8)}]g\rangle$$

$$
\begin{aligned}
&+O(v^2)|c\bar{c}[^1S_0^{(8)}]g\rangle + O(v^2)|c\bar{c}[^3S_1^{(1,8)}]gg\rangle \\
&+O(v^2)|c\bar{c}[^3P_J^{(1,8)}]gg\rangle + \cdots,
\end{aligned} \tag{2}
$$

where the $c\bar{c}$ pairs are indicated within the square brackets in spectroscopic notation. The pairs' color states are indicate by singlet (1) or octet (8) superscripts. The color octet $c\bar{c}$ states can make a transition into a physical J/ψ state by soft chromoelectric dipole ($E1$) transition(s) or chromomagnitic dipole ($M1$) transition(s)

$$
(c\bar{c})[^{2S+1}L_J^{(8)}] \rightarrow J/\psi. \tag{3}
$$

These color-octet contributions are essential for cancelling the logarithmic infrared divergences which appear in the color-singlet model calculations of the production cross sections and annihilation decay rates for P-wave charmonia, and for solving the ψ' and direct J/ψ "surplus" problems at the Fermilab Tevatron [13,14]. The NRQCD factorization scheme [15] has been established to systematically separate high- and low- energy scale interactions. Furthermore, NRQCD power counting rules can be exploited to determine the dominant contributions to various quarkonium processes [12]. For direct J/ψ production, the color-octet matrix elements, $\langle 0|\mathcal{O}_8^{J/\psi}[^3S_1]|0\rangle$, $\langle 0|\mathcal{O}_8^{J/\psi}[^1S_0]|0\rangle$ and $\langle 0|\mathcal{O}_8^{J/\psi}[^3P_J]|0\rangle$ are all scaling as $m_c^3 v_c^7$. So these color-octet contributions to J/ψ production must be included for consistency.

On the partonic level, associated $J/\psi+\gamma$ production are composed of the gluon fusion:

$$
\begin{aligned}
&g_1(p_1) + g(p_2) \rightarrow \gamma + (c\bar{c})[^3S_1^{(1)}, {}^3S_1^{(8)}] \ , \\
&g_1(p_1) + g(p_2) \rightarrow \gamma + (c\bar{c})[^1S_0^{(8)}, {}^3P_J^{(8)}] \ .
\end{aligned} \tag{4}
$$

The quark initiated subprocesses ($q\bar{q}$ channel) are strongly suppressed and will be neglected further. The color-singlet gluon-gluon fusion contribution to associated $J/\psi+\gamma$ production is well known [16]:

$$
\begin{aligned}
\frac{d\hat{\sigma}}{d\hat{t}}(\text{singlet}) = &\frac{1}{16\pi\hat{s}^2}\overline{\Sigma}|M(g+g\rightarrow\gamma+(c\bar{c})[^3S_1^{(1)}])|^2 \\
&\times\frac{1}{18m_c}\langle 0|\mathcal{O}_1^{J/\psi}[^3S_1]|0\rangle,
\end{aligned} \tag{5}
$$

where $\hat{s}=(p_1+p_2)^2$, $\langle 0|\mathcal{O}_1^{J/\psi}[^3S_1]|0\rangle$ is the color-singlet matrix element which is related to the lepton decay width of J/ψ in NRQCD

$$
\langle 0|\mathcal{O}_1^{J/\psi}[^3S_1]|0\rangle = \frac{\Gamma(J/\psi\rightarrow j^+l^-)m_c^2}{(2/9)\pi e_c^2\alpha^2}, \tag{6}
$$

where $e_c = 2/3$.

The average-squared amplitude of the subprocess $g+g\rightarrow\gamma+(c\bar{c})[^3S_1^{(8)}]$ can be obtained from the average-squared amplitude of $g+g\rightarrow\gamma+(c\bar{c})[^3S_1^{(1)}]$ by taking into account the defferent color factor. The result is

$$
\begin{aligned}
&\frac{d\hat{\sigma}}{d\hat{t}}[g+g\rightarrow\gamma+(c\bar{c})[^3S_1^{(8)}]\rightarrow\gamma+J/\psi] \\
&\quad=\frac{1}{16\pi\hat{s}^2}\frac{15}{6}\overline{\Sigma}|M(g+g\rightarrow\gamma+(c\bar{c})[^3S_1^{(1)}])|^2 \\
&\quad\times\frac{1}{24m_c}\langle 0|\mathcal{O}_8^{J/\psi}[^3S_1]|0\rangle.
\end{aligned} \tag{7}
$$

The average-squared amplitudes of the subprocesses $g+g\to\gamma+(c\bar{c})[^1S_0^{(8)}]$ and $g+g\to\gamma+(c\bar{c})[^3P_J^{(8)}]$ can be found in [17],

$$\begin{aligned}
&\frac{d\hat{\sigma}}{d\hat{t}}[g+g\to\gamma+(c\bar{c})[^1S_0^{(8)}]\to\gamma+J/\psi]\\
&\quad=\frac{1}{16\pi\hat{s}^2}\overline{\Sigma}|M(g+g\to\gamma+(c\bar{c})[^1S_0^{(8)}])|^2\\
&\quad\times\frac{1}{8m_c}\langle 0|\mathcal{O}_8^{J/\psi}[^1S_0]|0\rangle,\\
&\frac{d\hat{\sigma}}{d\hat{t}}[g+g\to\gamma+(c\bar{c})[^3P_J^{(8)}]\to\gamma+J/\psi]\\
&\quad=\frac{1}{16\pi\hat{s}^2}\sum_J\overline{\Sigma}|M(g+g\to\gamma+(c\bar{c})[^3P_J^{(8)}])|^2\\
&\quad\times\frac{1}{8m_c}\langle 0|\mathcal{O}_8^{J/\psi}[^3P_0]|0\rangle,
\end{aligned}\tag{8}$$

where the heavy quark spin symmetry

$$\langle 0|\mathcal{O}_8^{J/\psi}[^3P_J]|0\rangle=(2J+1)\langle 0|\mathcal{O}_8^{J/\psi}[^3P_0]|0\rangle\tag{9}$$

is exploited.

Now we consider the P_T distribution of J/ψ produced in process (1). Assuming hard diffractive factorization, the differential cross section can be expressed as

$$\begin{aligned}
d\sigma=&f_{\mathrm{I\!P}/p}(\xi_1)f_{\mathrm{I\!P}/\bar{p}}(\xi_2)f_{g/\mathrm{I\!P}}(x_1,Q^2)f_{g/\mathrm{I\!P}}(x_2,Q^2)\\
&\frac{d\hat{\sigma}}{d\hat{t}}[\text{singlet}+\text{octet}]d\xi_1d\xi_2dx_1dx_2d\hat{t},
\end{aligned}\tag{10}$$

where $\xi_1(\xi_2)$ is the momentum fraction of the proton (antiproton) carried by the Pomeron, $f_{g/\mathrm{I\!P}}(x_1,Q^2)$ is the gluon distribution function of the Pomeron, and $f_{\mathrm{I\!P}/p}(\xi)$ is the Pomeron flux factor integrated over t,

$$\begin{aligned}
f_{\mathrm{I\!P}/p}(\xi)&=\int_{-1}^{0}f_{\mathrm{I\!P}/p}(\xi,t)dt,\\
f_{\mathrm{I\!P}/p}(\xi,t)&=\frac{\beta_1^2(0)}{16\pi}\xi^{1-2\alpha(t)}F^2(t)\\
&=K\xi^{1-2\alpha(t)}F^2(t),
\end{aligned}\tag{11}$$

where the parameters are chosen as [18]

$$\begin{aligned}
K=0.73\ \text{GeV}^2,\quad&\alpha(t)=1+0.115+0.26\ (\text{GeV}^{-2})\ t,\\
F^2(t)=e^{4.6t}\ \ &(\text{valid at }|t|\le 1\ \text{GeV}^2).
\end{aligned}\tag{12}$$

For numberical predictions, we use $m_c=1.5$ GeV$,\Lambda_4=235$ MeV, and set the factoriztion scale and the renormalization scale both equal to the transverse mass of J/ψ, *i.e.*, $Q^2=m_T^2=(m_\psi^2+P_T^2)$, where P_T is the transverse momentum of J/ψ. For the color-octet matrix elements $\langle 0|\mathcal{O}_8^{J/\psi}[^3S_1]|0\rangle$, $\langle 0|\mathcal{O}_8^{J/\psi}[^1S_0]|0\rangle$, and $\langle 0|\mathcal{O}_8^{J/\psi}[^3P_0]|0\rangle$ we use the values determined by Beneke and Krämer [19] from fitting the direct J/ψ production data at the Tevatron [13] using GRV LO parton distribution functions [20]:

$$\begin{aligned}\langle 0|\mathcal{O}_8^{J/\psi}[^3S_1]|0\rangle &= 1.12 \times 10^{-2}\ \mathrm{GeV}^3,\\ \langle 0|\mathcal{O}_8^{J/\psi}[^1S_0]|0\rangle + \frac{3.5}{m_c^2}\langle 0|\mathcal{O}_8^{J/\psi}[^3P_0]|0\rangle &= 3.90 \times 10^{-2}\ \mathrm{GeV}^3. \end{aligned} \tag{13}$$

The matrix elements $\langle 0|\mathcal{O}_8^{J/\psi}[^1S_0]|0\rangle$ and $\langle 0|\mathcal{O}_8^{J/\psi}[^3P_0]|0\rangle$ are not determined separately, so we present the two extreme values allowed by Eq.(13) as

$$\begin{aligned} {}^1S_0 \text{ saturated case :}&\langle 0|\mathcal{O}_8^{J/\psi}[^1S_0]|0\rangle = 3.90 \times 10^{-2}\ \mathrm{GeV}^3\\ &\langle 0|\mathcal{O}_8^{J/\psi}[^3P_0]|0\rangle = 0,\\ {}^3P_J \text{ saturated case :}&\langle 0|\mathcal{O}_8^{J/\psi}[^3P_0]|0\rangle = 1.11 \times 10^{-2} m_c^2\ \mathrm{GeV}^3\\ &\langle 0|\mathcal{O}_8^{J/\psi}[^1S_0]|0\rangle = 0. \end{aligned} \tag{14}$$

We use the hard gluon distribution function for the Pomeron [6]:

$$x f_{g/\mathbb{P}}(x, Q^2) = f_g 6x(1-x),\ \ f_g = 0.7. \tag{15}$$

We neglect any Q^2 evolution of the gluon density of the Pomeron at present stage. As usual, in order to suppress the Reggon contributions, we set $\xi_1, \xi_2 \leq 0.05$.

With all ingredients set as above, the P_T distribution of J/ψ can be calculated in a standard way from Eq. (10). In Fig. 1 we show the P_T distribution $Bd\sigma/dP_T$ for associated $J/\psi + \gamma$ production through DPE in $p\bar{p}$ collisions at $\sqrt{s} = 1.8$TeV , integrated over the pseudo-rapidity region $-1 \leq \eta \leq 1$ (the central region). Where $B = 0.0594$ is the $J/\psi \rightarrow \mu^+\mu^-$ leptonic decay branching ratio. The lowest solid line is the color-singlet gluon-gluon fusion contribution, while the lowest dashed, dotted lines are ${}^1S_0^{(8)}$-saturated, and ${}^3S_1^{(8)}$ color-octet contributions respectively. The ${}^3P_J^{(8)}$-saturated color-octet contribution is almost the same as the ${}^1S_0^{(8)}$-saturated case, so we don't show it in the figure, and we don't consider it further. For comparision, we also show the P_T distribution of J/ψ produced in the inclusive process $p + \bar{p} \rightarrow J/\psi + \gamma + X$ and the single diffractive process $p + \bar{p} \rightarrow \bar{p} + J/\psi + \gamma + X$ in the same kinematic region, the results are shown as the upper and middle lines of Fig. 1. The code for the lines is the same as the DPE case. As shown in Fig. 1, the color-octet ${}^3S_1^{(8)}$ contribution is strongly suppressed compared with the others over the entire P_T region considered. The ${}^1S_0^{(8)}$ -saturated contribution is smaller than the singlet contribution where $P_T \leq 5$ GeV. Integrated over the P_T region ($2.0 \leq P_T \leq 5.0$GeV), the color-singlet, ${}^1S_0^{(8)}$-saturated, and ${}^3S_1^{(8)}$ contributions to $B\sigma^{\mathrm{DPE}}$ are 0.47, 0.12, and 1.4×10^{-2} pb respectively. The total cross section times the leptonic decay branching ratio of $J/\psi B$ at $\sqrt{s} = 1.8$TeV, integarated over the same P_T and η region for DPE, SD, and inclusive production of associated $J/\psi + \gamma$ are 0.60, 19, and 4.0×10^2 pb respectively. The ratios of the total DPE and SD cross sections to that of inclusive production in the central region are $R^{\mathrm{DPE}} = 1.5 \times 10^{-3}$ and $R^{\mathrm{SD}} = 4.8 \times 10^{-2}$ respectively.

In Fig. 2, we show the P_T distribution of J/ψ, $Bd\sigma/dP_T$, integrated over the same pseudo-rapidity region at the CERN LHC energy $\sqrt{s} = 14$ TeV for the inclusive, SD, and

DPE processes, the code for the lines is the same as Fig. 1. Integrated over the P_T region ($2.0 \leq P_T \leq 5.0$GeV), the color-singlet, ${}^1S_0^{(8)}$-saturated, and ${}^3S_1^{(8)}$ contributions to $B\sigma^{\rm DPE}$ are 1.2, 0.30, and 3.6×10^{-2} pb respectively. The total cross section times the leptonic decay branching ratio of $J/\psi B$ at $\sqrt{s} = 14$TeV, integarated over the same P_T and η region for DPE, SD, and inclusive production of associated $J/\psi + \gamma$ are 1.6, 88, and 3.1×10^3 pb respectively. The ratios of the total DPE and SD cross sections to that of inclusive production in the central region are $R^{\rm DPE} = 5.2 \times 10^{-4}$ and $R^{\rm SD} = 2.8 \times 10^{-2}$ respectively. We have varied the color-octet matrix elements $\langle 0|\mathcal{O}_8^{J/\psi}[{}^1S_0]|0\rangle + \frac{3.5}{m_c^2}\langle 0|\mathcal{O}_8^{J/\psi}[{}^3P_0]|0\rangle$ and $\langle 0|\mathcal{O}_8^{J/\psi}[{}^3S_1]|0\rangle$ by multiplied them by a factor between 1/10 and 2, the ratios $R^{\rm DPE}$ and $R^{\rm SD}$ above are unvaried. This character demonstrates that the ratios $R^{\rm DPE}$ and $R^{\rm SD}$ are insensitive to the values of color-octet matrix elements.

In TABLE I., we show the ratios

$$R^{\rm DPE}(P_T) = \frac{d\sigma^{\rm DPE}}{dP_T} / \frac{d\sigma^{\rm Inclusive}}{dP_T},$$
$$R^{\rm SD}(P_T) = \frac{d\sigma^{\rm SD}}{dP_T} / \frac{d\sigma^{\rm Inclusive}}{dP_T} \tag{16}$$

at $\sqrt{s} = 1.8$ and 14 TeV in the central rapidity region.

From this table, we can see that $R^{\rm SD}(P_T)$ is almost constant for the P_T region considered, so $R^{\rm SD}$ is insensitive to the P_T smearing effects. But $R^{\rm DPE}(P_T)$ varies rapidly with P_T, from 2 GeV to 5 GeV, which decreases by almost one order, so $R^{\rm DPE}$ is sensitive to the P_T smearing effects, this can be attributed to the limited production phase space and an additional hard gluon distribution of the Pomeron in the DPE compared with the SD case.

In the above calculation, we use the standard Pomeron flux factor (valid at small t) that appears in the triple-Pomeron amplitude for SD. In order to preserve the shapes of the M^2 and t distribution in soft single diffraction and predict correctly the experimentally observed SD cross section at all energies in $p - \bar{p}$ collisions, Goulianos [18] proposed to renormalize the Pomeron flux in an energy-dependent way:

$$f_{\mathbb{P}/p}^{\rm RN}(\xi, t) = D f_{\mathbb{P}/p}(\xi, t), \tag{17}$$

the renormalization factor D is defined as

$$D = \min(1, \frac{1}{N}) \tag{18}$$

with

$$N = \int_{\xi_{\rm min}}^{\xi_{\rm max}} d\xi \int_{-\infty}^{0} dt f_{\mathbb{P}/p}(\xi, t), \tag{19}$$

where $\xi_{\rm min} = M_0^2/s$ with $M_0^2 = 1.5{\rm GeV}^2$(effective threshold) and $\xi_{\rm max} = 0.1$(coherence limit). For $\sqrt{s} = 1.8, 14$ TeV, the renormalization factor $D = 0.11, 5.2 \times 10^{-2}$ respectively. Furthermore, by comparing the CDF data on diffractive W production with predictions using the Pomeron structure function measured at HERA, Goulianos concluded that the breakdown of hard diffractive factorization in hadron-hadron collisions is due to the breakdown of the Regge factorization already observed in soft diffraction [21]. In this picture, the renormalization factor D indicates the factorization broken effects and takes the role of the survival probability for hadron emerges from the diffractive collision intact [22]. Using the renormalized Pomeron flux factor, the P_T distribution calculated above must be multiplied by a factor D^2 and D for DPE and SD case respectively, therefore, the ratio $R^{\rm DPE}$ and $R^{\rm SD}$ are proportional to $D^2 f_g^2$ and Df_g respectively , hence they are sensitive to the gluon fraction of the Pomeron f_g and the renormalization factor D which indicates the factorization broken effects. From other diffractive production experiments, f_g can be determined, the renormalization factor D can be determined precisely from those ratios, and *vice versa*. So measuring these ratios can probe the gluon density in the Pomeron and shed light on the nature of hard diffractive factorization breaking. Furthermore, sence $R^{\rm DPE}$ is sensitive to the P_T smearing effects, the experimental study of associated $J/\psi + \gamma$ production through DPE can give valuble information about the P_T smearing effects which are needed to solve the large-z discrepancy seen by comparing NRQCD predictions with the HERA data on inelastic J/ψ photoproduction [23].

Experimentally, the nondiffractive background to the diffractive associated $J/\psi + \gamma$ production must be dropped out in order to obtain useful information, this can be attained by performing the rapid gap analysis or using the Forward Proton Detector.

In conclusion, in this BRIEF REPORT we have shown that diffractive associated $J/\psi+\gamma$ production at large P_T is sensitive to the gluon content of the Pomeron and the factorization broken effects in hard diffraction. Although the diffractive and inclusive production cross sections are sensitive to the values of coler-octet matrix elements, the ratioa of the diffractive to inclusive $J/\psi+\gamma$ production are not so and proportional to $D^2 f_g^2$ and Df_g for DPE and SD case respectively, hence they are sensitive to the gluon fraction of the Pomeron and the the factorization broken effects. So experimental measurement of these ratios at the Tevatron and LHC can shed light on the nature of Pomeron and hard diffractive factorization breaking. Furthermore, sence the ratio of the total DPE cross section to that of inclusive production is sensitive to the P_T smearing effects, the experimental study of associated $J/\psi+\gamma$ production through DPE can give valuble information about the P_T smearing effects.

Acknowledgments

This work is supported in part by the National Natural Science Foundation of China, Doctoral Program Foundation of Institution of Higher Education of China and Hebei Natural Province Science Foundation, China.

REFERENCES

[1] P. D. B. Collins, *An introduction to Regge theory and High Energy Physics* , Cambridge University Press, Cambridge, England, 1977; K. Goulianos, Phys. Rep. **101**, 169 (1985).

[2] G. Ingelman and P. E. Schlein, Phys. Lett. B **152**, 256 (1985).

[3] UA8 Collaboration, A. Brandt *et al.*, Phys. Lett. B **297**, 417 (1992) ; R. Bonino *et al.*, *ibid.* **211**, 239 (1988).

[4] ZEUS Collaboration, M. Derrick *et al.*, Z. Phys. C **68**, 569 (1995) ; Phys. Lett. B **356**, 129 (1995).

[5] H1 Collaboration, T. Ahmed *et al.*, Phys. Lett. B **348**, 681 (1995) ; C. Adloff *at al.*, Z. Phys. C **76**, 613 (1997); For a recent review on diffraction at HERA, see P. Marage, hep-ph/9810551.

[6] CDF Collaboration, F. Abe *et al.*, Phys. Rev. Lett. **78**, 2698 (1997); **79**, 2636 (1997).

[7] J. C. Collins, Phys. Rev. D **57**, 3051 (1998).

[8] J. C. Collins, L. Frankfurt, and M. Strikmam, Phys. Lett. B **307**, 161 (1993); A. Berera and D. E. Soper, Phys. Rev. D **50**, 4328 (1994).

[9] L. Alvero, J. C. Collins, J. Terron, and J. J. Whitmore, hep-ph/9805268; L. Alvero, J. C. Collins, and J. J. Whitmore, hep-ph/9806340.

[10] Jia-Sheng Xu and Hong-An Peng, Phys. Rev. D **59** (1), (1999).

[11] W. E. Caswell and G. P. Lepage, Phys. Lett. B **167**, 437 (1986).

[12] G. P. Lepage, L. Magnea, C. Nakhleh, U. Magnea, and K. Hornbostel, Phys. Rev. D **46**, 4052 (1992).

[13] CDF Collaboration, F. Abe *et al.*, Phys. Rev. Lett. **79**, 572 (1997); **79**, 578 (1997).

[14] For some recent reviews, see E. Braaten, S. Fleming, and T.C. Yuan, Annu. Rev. Nucl. Part. Sci. **46**, 197 (1996); hep-ph/9602374 ; E. Braaten, hep-ph/9702225; hep-ph/9810390; M. Beneke, hep-ph/9703429; and references therein.

[15] G. T. Bodwin, E. Braaten, and G. P. Lepage, Phys. Rev. D **51**, 1125 (1995); **55**, 5853(E) (1997).

[16] E. L. Berger and D. Jones, Phys. Rev. D **23**, 1512 (1981); R. Baier and R. Rukel, Z. Phys. C **19** 251 (1983).

[17] C. S. Kim, Jungil Lee, and H.S. Song, Phys. Rev. D **55**, 5429 (1997); P. Ko, Jungil Lee, and H.S. Song, *ibid.*, **54**, 4312 (1996).

[18] K. Goulianos, Phys. Lett. B **358**, 379 (1995); **363**, 268(E) (1995) ; K. Goulianos and J. Montanha, hep-ph/9805496.

[19] M. Beneke and M. Krämer, Phys. Rev. D **55**, R5269 (1997).

[20] M. Glück, E. Reya, and A. Vogt, Z. Phys. C **67**, 433 (1995).

[21] K . Goulianos, hep-ph/9708217.

[22] D. E. Soper, hep-ph/9707384.

[23] H1 Collaboration, S. Aid *et al.*, Phys. Lett. B **472**, 3 (1996); ZEUS Collaboration, J. Breitweg *et al.*, hep-ex/9708010; B. Cano-Coloma and M. A. Sanchis-Lozano, Nucl. Phys. **B508**, 753 (1997); B. A. Kniehl and G. Kramer, hep-ph/9803256; K. Sridhar, A. D. Martin, and W. J. Stirling, hep-ph/9806253.

Figure Captions

Fig. 1. Transverse momentum of $J/\psi(P_T)$ distribution $Bd\sigma/dP_T$, integrated over the J/ψ pseudo-rapidity range $|\eta| \leq 1$ (central region), for associated $J/\psi + \gamma$ production through double Pomeron exchange (lower), in single diffractive (middle), and inclusive (upper) processes at the Tevatron ($\sqrt{s} = 1.8$ TeV). Here B is the branching ratio of $J/\psi \to \mu^+\mu^-(B = 0.0594)$. The solid line is the color-singlet gluon-gluon fusion contribution, the dashed line represents ${}^1S_0^{(8)}$-saturated color-octet contribution, the dotted one is ${}^3S_1^{(8)}$ color-octet contribution. The inclusive and single production data are multiplied by a factor 100 and 10 respectively. Fig. 2. Transverse momentum of $J/\psi(P_T)$ distribution $Bd\sigma/dP_T$, integrated over the J/ψ pseudo-rapidity range $|\eta| \leq 1$ (central region), for associated $J/\psi + \gamma$ production through double Pomeron exchange (lower), in single diffractive (middle), and inclusive (upper) processes at the CERN LHC ($\sqrt{s} = 14$ TeV). Here B is the branching ratio of $J/\psi \to \mu^+\mu^-(B = 0.0594)$. The solid line is the color-singlet gluon-gluon fusion contribution, the dashed line represents ${}^1S_0^{(8)}$-saturated color-octet contribution, the dotted one is ${}^3S_1^{(8)}$ color-octet contribution. The inclusive and single production data are multiplied by a factor 100 and 10 respectively.

TABLES

TABLE I. The ratio $R^{\mathrm{SD}}(P_T)$, $R^{\mathrm{DPE}}(P_T)$ as a function of P_T at the Tevatron and LHC energies in central region ($-1 \leq \eta \leq 1$) using the standard Pomeron flux (D = 1.0).

P_T (GeV)	2.0	2.5	3.0	3.5	4.0	4.5	5.0
$R^{\mathrm{SD}}(P_T)$ ($\sqrt{s} = 1.8$ TeV) (10^{-2})	4.9	4.9	4.8	4.8	4.7	4.7	4.7
$R^{\mathrm{SD}}(P_T)$ ($\sqrt{s} = 14$ TeV) (10^{-2})	2.9	2.9	2.9	2.9	2.9	2.9	2.9
$R^{\mathrm{DPE}}(P_T)$ ($\sqrt{s} = 1.8$ TeV) (10^{-3})	2.0	1.7	1.3	1.0	0.71	0.46	0.25
$R^{\mathrm{DPE}}(P_T)$ ($\sqrt{s} = 14$ TeV) (10^{-4})	6.9	5.8	4.5	3.3	2.2	1.1	0.23

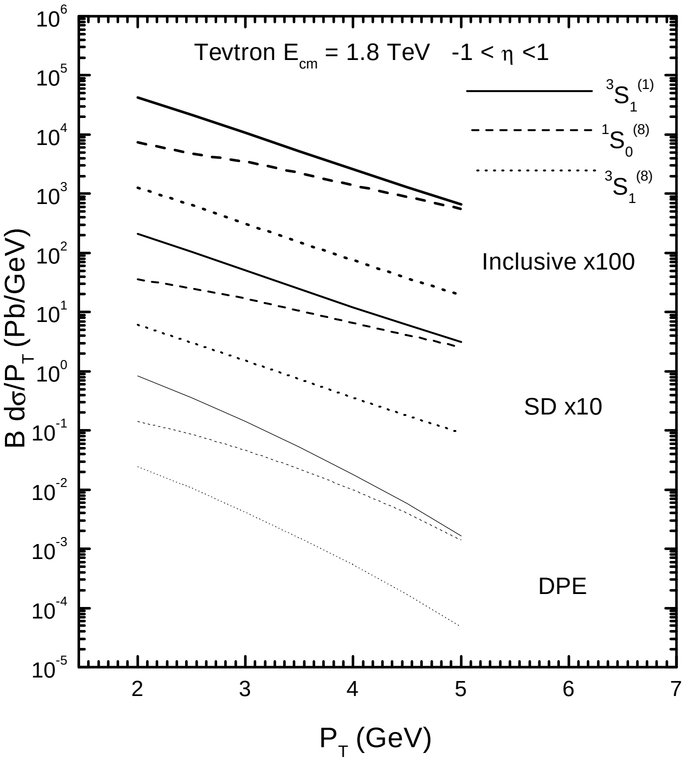
Tevtron E_{cm} = 1.8 TeV -1 < η <1
$^3S_1^{(1)}$
$^1S_0^{(8)}$
$^3S_1^{(8)}$
Inclusive x100
SD x10
DPE
B dσ/P_T (Pb/GeV)
10^6
10^5
10^4
10^3
10^2
10^1
10^0
10^{-1}
10^{-2}
10^{-3}
10^{-4}
10^{-5}
2
3
4
5
6
7
P_T (GeV)

Fig. 1

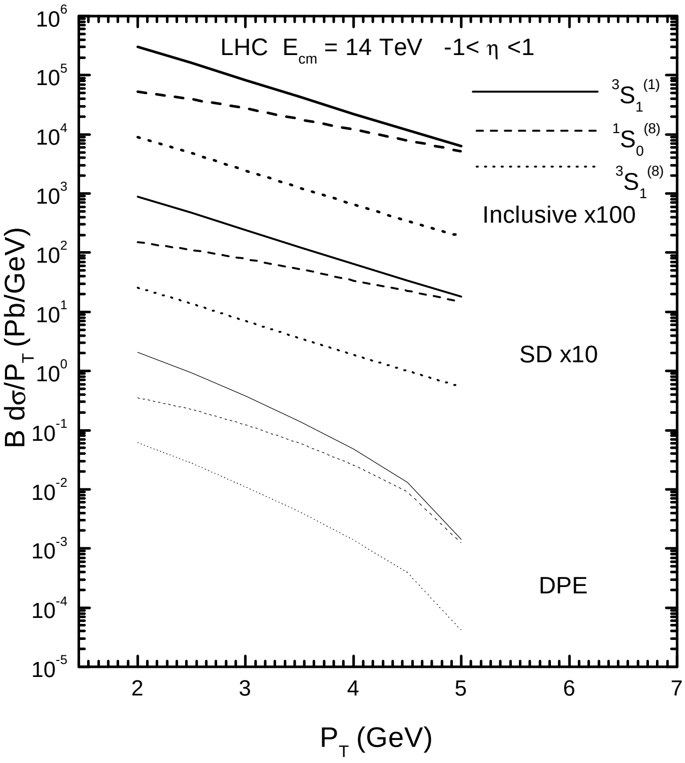
LHC E_{cm} = 14 TeV -1< η <1
$^3S_1^{(1)}$
$^1S_0^{(8)}$
$^3S_1^{(8)}$
Inclusive x100
SD x10
DPE
B dσ/P_T (Pb/GeV)
P_T (GeV)
10^6
10^5
10^4
10^3
10^2
10^1
10^0
10^{-1}
10^{-2}
10^{-3}
10^{-4}
10^{-5}
2
3
4
5
6
7

Fig. 2